Implant Dopant Activation Comparison Between Silicon and Germanium

John O. Borland and Paul T. Konkola
Advanced Integrated Photonics
435 Keawe St.
Honolulu, Hawaii, 96813, USA

***Abstract*—We report room temperature p-type acceptor formation in Ge from B and C implant damage up to a level of 120Ω/□ or 1E19/cm^3. For n-type dopant implants in Ge we found that an oxide surface capping layer was required above 625^{o}C to prevent dopant surface loss. P followed by As then Sb gave the best dopant activation and at the same low temperature anneal B, P, As and Sb Rs values were always lower in Ge by 1.3x to 3x than in Si possibly directly related to the higher mobility ratio in Ge to Si and differences in Ge dopant surface loss and segregation into oxide.**

***Keywords*—germanium; phosphorus; arsenic; antimony; boron; rapid thermal annealing; laser annealing; solid solubility**

I. INTRODUCTION

Embedding Si-CMOS technology with localized regions of 80-100% Ge material for high mobility channels will start to occur at the 10nm node and beyond for both pMOS and nMOS devices. Poor n-type dopant activation with rapid diffusion has been reported for the past decade as one of the limitation for Ge-NFET devices as reported by Saraswat [1] in 2005. However, in 2009 Kim et al [2] reported using co-implants of P+Sb to achieve >1E20/cm^3 n-type dopant activation in Ge. The historical dopant solid solubility limit comparative data for Si and Ge was reported by Trumbore [3] dating back to 1959 is missing data for B and P in Ge and only shows solid solubility data for p-type Ga dopant starting at 24^{o}C (room temperature) and n-type As starting at 750^{o}C and Sb starting at 600^{o}C. In Si the solid solubility data for B starts at 1150^{o}C, As at 1075^{o}C, P at 900^{o}C and Sb at 700^{o}C. Therefore, we decided to do an up to date direct comparison of implanted dopant activation in Si and Ge materials from room temperature to the melting temperature of Ge at 937^{o}C and Si at 1407^{o}C using RTA and laser annealing.

II. EXPERIMENTATION

A. P-type Implantation

For p-type implantation we used 150mm Cz bulk Si n(100) and Ge n(100) wafers. B was implanted at 30keV and either a dose of 5E15/cm^2 or 5E14/cm^2. We also used BF$_2$ implantation at 150keV, 5E14/cm^2 dose to investigate the effects of a self-amorphizing implant on dopant activation. RTA annealing for 10 sec from 400^{o}C to 900^{o}C for the Ge implanted wafers and from 700^{o}C to 1050^{o}C for the Si implanted wafers. Laser melt annealing was also performed.

B. N-type Implantation

For n-type implantation we used 150mm Cz bulk Si p(100) wafers and grew 1um of intrinsic Ge-epilayer on top. We also compared two doses at 1E16/cm^2 and 2E15/cm^2 for phosphorus (P) dopant but only 1E16/cm^2 for arsenic (As) and antimony (Sb) dopants all at 20keV. We also investigated co-implants of P+Sb, P+F and P+C. The p-type and n-type implant matrix is listed in Table I below.

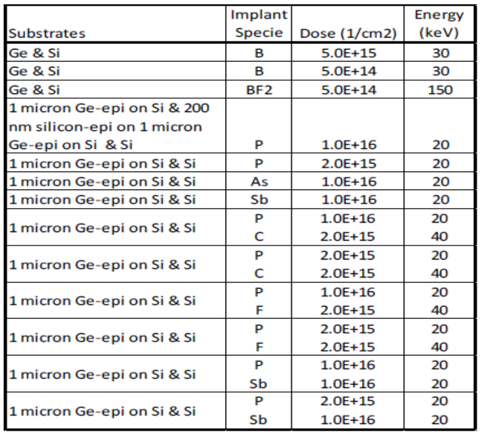

Substrates	Implant Specie	Dose (1/cm2)	Energy (keV)
Ge & Si	B	5.0E+15	30
Ge & Si	B	5.0E+14	30
Ge & Si	BF2	5.0E+14	150
1 micron Ge-epi on Si & 200 nm silicon-epi on 1 micron Ge-epi on Si & Si	P	1.0E+16	20
1 micron Ge-epi on Si & Si	P	2.0E+15	20
1 micron Ge-epi on Si & Si	As	1.0E+16	20
1 micron Ge-epi on Si & Si	Sb	1.0E+16	20
1 micron Ge-epi on Si & Si	P C	1.0E+16 2.0E+15	20 40
1 micron Ge-epi on Si & Si	P C	2.0E+15 2.0E+15	20 40
1 micron Ge-epi on Si & Si	P F	1.0E+16 2.0E+15	20 40
1 micron Ge-epi on Si & Si	P F	2.0E+15 2.0E+15	20 40
1 micron Ge-epi on Si & Si	P Sb	1.0E+16 1.0E+16	20 20
1 micron Ge-epi on Si & Si	P Sb	2.0E+15 1.0E+16	20 20

Table I. Detailed implant matrix investigated.

III. RESULTS

A. B and BF$_2$ Implants into Ge and Si

The Rs (sheet resistance) results measured by 4PP after the various p-type implants before and after annealing are shown in Fig.1 below. Note most interesting is the self-activation (decrease in Rs) of p-type dopant after implant especially for monomer B as the dose increases. Using 4PP measurement the 5E14/cm^2 B-implant Rs was 190Ω/□ and at higher implant dose of 5E15/cm^2 Rs was 120Ω/□ suggesting the implant damage in Ge creates acceptors/holes equivalent to an implant B dose of 1E14/cm^2. When BF$_2$ implant was used which is self-amorphizing with less residual implant damage the Rs was much higher at 680Ω/□. Similar self-activation (acceptor formation) implants into Ge was also observed by others [4,5]. At an RTA temperature of 450^{o}C the self-amorphizing BF$_2$ implant was fully activated by SPE (solid phase epitaxy). B required temperatures >600^{o}C for full activation. But with laser melt annealing B deactivation was observed as the Rs increased from 17Ω/□ at 900^{o}C to 55Ω/□ at 950^{o}C melt anneal.

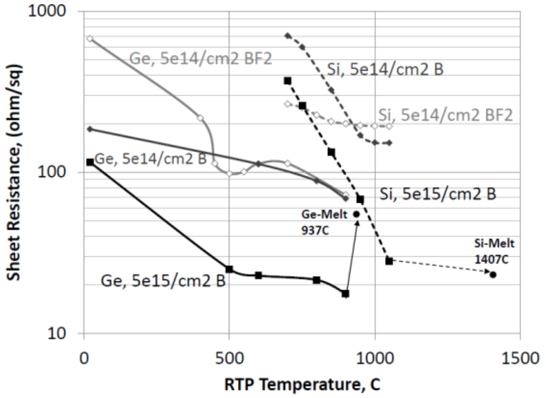

Fig.1. 4PP Rs versus anneal temperature for B and BF$_2$ implants.

Results for Si are as expected in Fig.1 above. SPE activation for BF$_2$ 5E14/cm^2 was observed at 700^{o}C with an Rs value of 265Ω/□ with full activation saturation by 900^{o}C and Rs of 200Ω/□. B Rs was 700Ω/□ at 700^{o}C and fully activated to 140Ω/□ by 1000^{o}C. Increasing the B dose 10x to 5E15/cm^2 reduced Rs to 380Ω/□ at 700^{o}C requiring higher anneal temperatures for full B activation above 1050^{o}C and Rs of 27Ω/□. With laser melt >1407^{o}C Rs was 22Ω/□.

The >10x lower boron dopant Rs in Ge compared to Si over the temperature range from 500^{o}C to 800^{o}C is clearly evident in Fig.1 and is partially due to the 3-4x higher hole mobility in Ge than Si and also higher B dopant solid solubility in Ge at these lower temperatures assuming 100% retained implant dose. But Ge laser melt annealing resulted in B deactivation to the 55Ω/□ level, similar poor B laser melt activation was also reported by Mazzocchi [6] in 2009. Fig, 2 below plots various B activation Rs values versus B implant dose for our results along with the results from several others including Impellizzeri [7] and Borland [8]. The dot-line is the lowest Rs values for Ge while the dash-line is for Si and at low B dose of 1E14/cm^2 this difference is 2.1x and at the higher dose of 1E16/cm^2 is reduced to 1.3x possibly reflecting differences in mobility with high dopant levels.

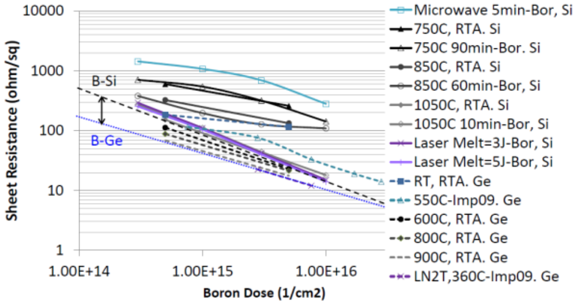

Fig.2. Rs versus B implant dose for various activation levels.

SRP of the self-activation (acceptor formation) B implant at 5E15/cm^2 (120Ω/□) is shown in Fig.3. The p-type acceptor carrier level is ~1E19/cm^3 to a depth of 0.4um with no annealing. Note the increased in B carrier activation with RTA annealing temperature but deactivation with laser melt annealing. The SRP absolute carrier density level may not be accurate due to resistivity calibration and mobility differences between Si and Ge as reported by Clarysse [9] but the trends in data are accurate.

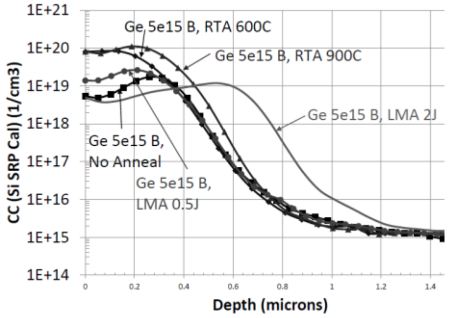

Fig.3. SRP of B 5E15/cm^2 after RTA annealing and laser melt annealing.

B. P, As and Sb Implants into Ge and Si and co-implants of P+Sb, P+F and P+C into Ge

Results for phosphorus implant at 2E15/cm^2 and 1E16/cm^2 dose and without a surface oxide capping layer are shown in Fig.4. The wafer with exposed Ge surface with 1E16/cm^2 P-implant showed activation saturation after 700^{o}C anneal and slight dopant loss after 900^{o}C anneal. Oh [10] reported about 100nm loss of Ge from the surface after 600^{o}C RTP annealing therefore we added a 500nm PECVD-oxide surface capping layer which resulted in the improved P Rs values down to 9Ω/□ at 900^{o}C. A surface oxide capping layer was used for all the subsequent anneals. The 2E15/cm^2 P-implant reaches full dopant activation at 625^{o}C with Rs saturation of 45Ω/□ but increased to 55Ω/□ at 900^{o}C.

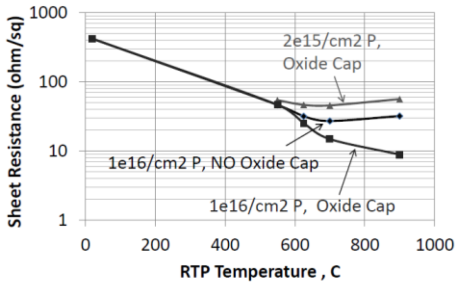

Fig.4. P Rs versus RTA temperature for 2E15/cm^2 and 1E16/cm^2 dose and without oxide surface caping layer.

Comparison between P, As and Sb implanted dopants at 1E16/cm^2 into both Si wafer and 1um Ge-epilayer on Si after various RTA anneals are shown in Fig.5 below. Similar to what we observed for B in Fig.1, the Rs values for all three n-type dopants were always lower in Ge than in Si over the temperature range from 625^{o}C to 900^{o}C by about 5x for P and 10x for As and Sb. In Ge over the temperature range investigated the solid solubility limit of P is always the highest followed by As with Sb being the lowest, this is also for Si. Fig.6 includes the results for co-implants of P+Sb, P+C and P+F as well as into a Si-cap layer to verify if we also see an enhanced n-type dopant activation in Ge with P+Sb as reported by Kim [2] and Thareja [11] along with reduced P diffusion with P+F or P+C co-implants. Our Rs results do not show any enhanced n-type dopant activation with co-implants, F has no effect but C clearly results in higher Rs so the C-implant damage creates more acceptors similar to B which compensates the P n-type dopants especially at the lower anneal temperatures. Sb co-implants also results in higher Rs with P at the higher annealing temperatures.

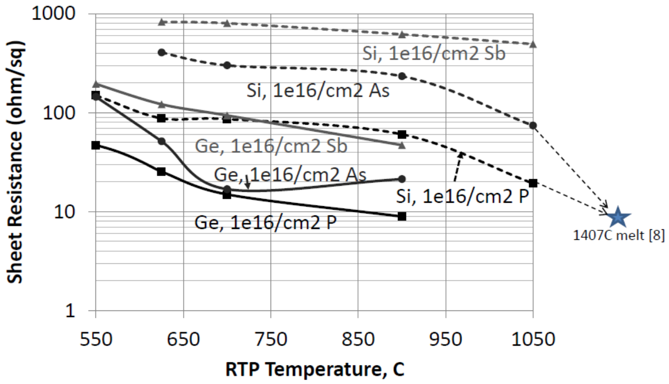

Fig.5. Rs versus RTA annealing temperatures for P, As and Sb implanted dopants into Ge and Si.

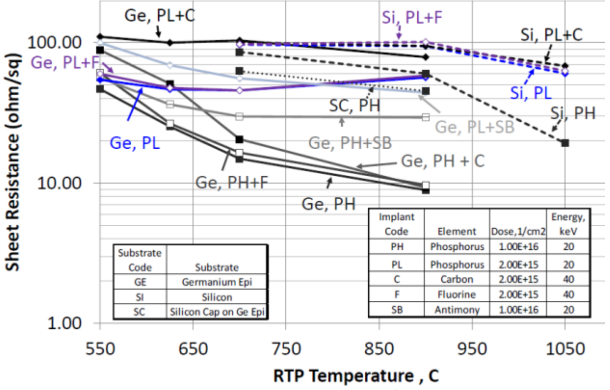

Substrate Code	Substrate
GE	Germanium Epi
SI	Silicon
SC	Silicon Cap on Ge Epi

Implant Code	Element	Dose,1/cm2	Energy, keV
PH	Phosphorus	1.00E+16	20
PL	Phosphorus	2.00E+15	20
C	Carbon	2.00E+15	40
F	Fluorine	2.00E+15	40
SB	Antimony	1.00E+16	20

Fig.6. Rs versus RTA annealing temperatures for P+Sb, P+C and P+F co-implants into Ge and Si.

Fig. 7 below plots n-type dopant Rs versus implanted dose in Si and Ge with the dash line for 100% full dopant activation in Si with data from several other reports [6,8,11]. Some of the Ge-P results were below the n-type Si line so in Table II we report the P-SIMS retained dose values in Ge after anneal and observed significant P dopant loss even though we used an oxide cap suggesting dopant segregation into the oxide capping layer. In some cases only 6% of the P dose was retained so replot of Rs versus P-retained dose is shown in Fig.8. The new plot shows P dopant Rs in Ge is actually 4.3x to 3.2x lower than in Si and at an n-type doping level of 5E19/cm^3 the electron mobility in Ge is only 2.5x higher than in Si so the additional difference could be related to higher P dopant solid solubility limit in Ge.

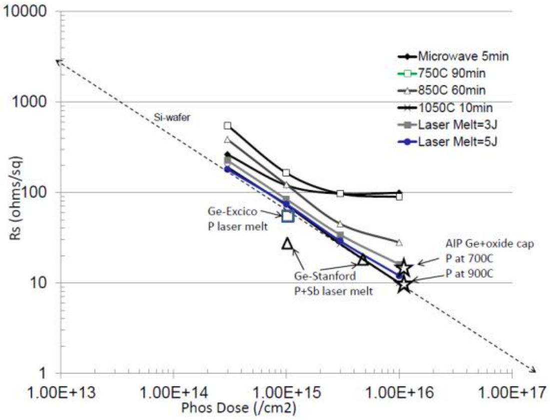

Fig.7. Rs versus P-implant dose in Si and Ge.

Specie Assessed	P	P	P	P	P
Temperature	SiCap, 1e16P/cm2	Ge, 1e16P/cm2	Ge, 2e15P/cm2	Ge, 2e15P/cm2+ 2e15C/cm2	Ge, 2e15P/cm2+ 2e15F/cm2
625	86%	14%	18%		
900	78%	23%	7%	9%	6%
950			34%		

TableII. SIMS measured P retained dose in Ge after anneal.

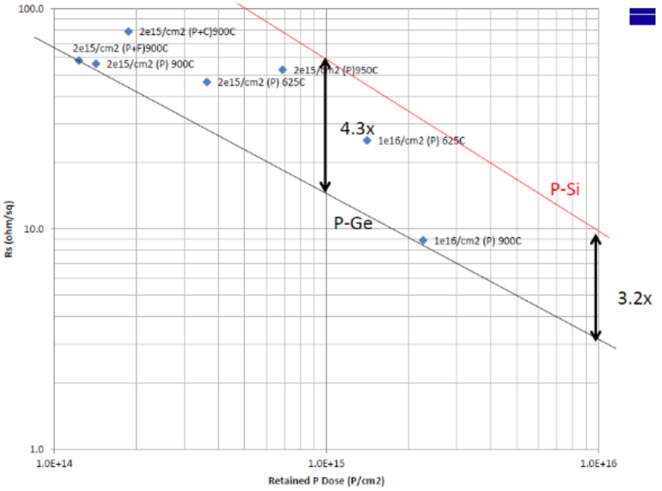

Fig.8. Corrected Rs versus P-retained dose in Ge.

SRP for the for the As-implant wafers after 625°C and 900°C RTA anneals are shown in Fig.9 below. Rapid As diffusion is seen in Ge at 900°C and significant deactivation with 950°C melt anneal. Si and Ge SIMS revealed a uniform Si incorporation level of 10% in the Ge-epilayer after the 950°C melt anneal which is the solid solubility level of Si in Ge at that temperature. Similarly SRP results for Sb-implants are shown in Fig. 10 below. Fig. 11 compares P-implant to co-implants of P+F and P+C in Ge at 625°C along with the use of a 0.2um Si-capping layer ontop of the Ge-epi while Fig.12 is for 900°C anneal where rapid P-diffusion is observed. Note that in Fig.11 with the C co-implant the SRP carrier density level is about 1E19/cm^3 lower than without C co-implant consistent with the 1E19/cm^3 acceptor level created by the B-implant damage shown in Fig. 3 which is compensating the n-type dopant region. Also note that with the Si-cap a 900°C anneal can be used with minimal P-diffusion in Ge maintaining high P dopant activation. Another benefit of the high temperature 900°C RTA anneal is the reduction in Ge-epi threading dislocation compared to 625°C as shown in the X-TEMs of Fig.13.

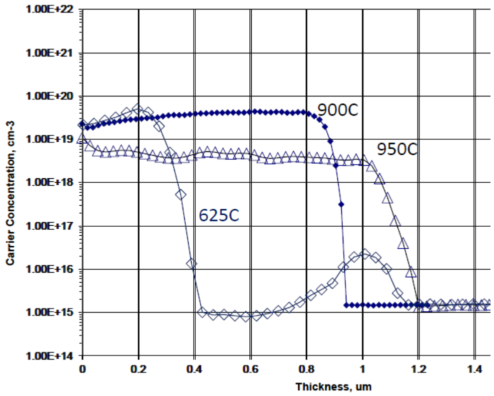

Fig.9. SRP for As-implant 1um Ge-epi wafers after RTA annealing.

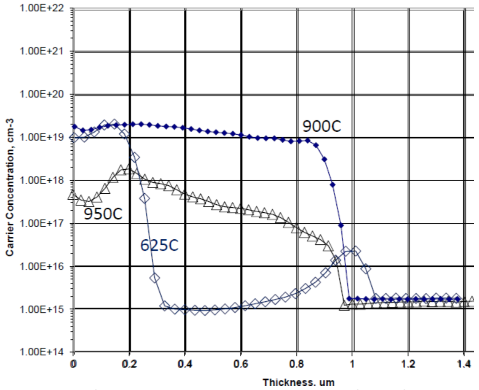

Fig.10. SRP for Sb-implant 1um Ge-epi wafers after RTA annealing.

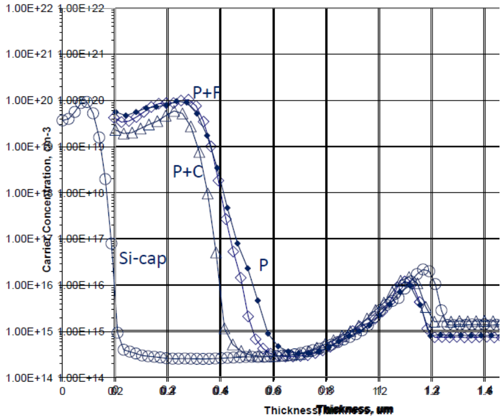

Fig.11. SRP for P-implant and co-implant in 1um Ge-epi wafers after 625ºC RTA annealing.

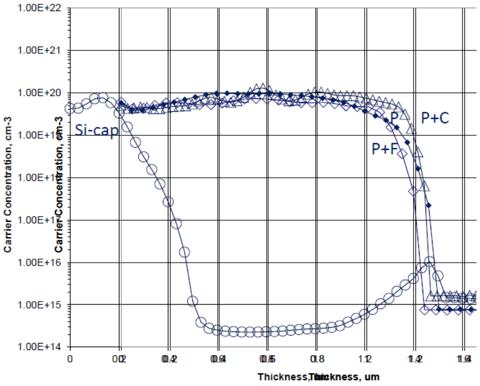

Fig.12. SRP for P-implant and co-implant in 1um Ge-epi wafers after 900ºC RTA annealing.

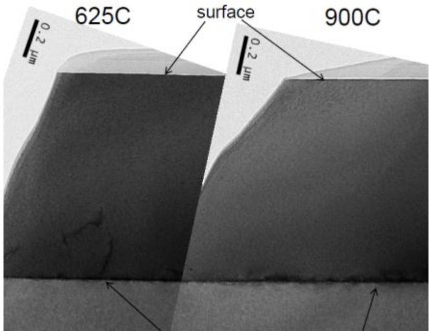

Fig.13. X-TEM of 1um Ge-epi after 625ºC, 900ºC and 950ºC RTA anneal.

IV. SUMMARY

We observed room temperature formation of p-type acceptors in Ge from B and C implant damage up to a level of 120Ω/□ or 1E19/cm^3. This was not observed with a BF$_2$ self-amorphizing implant. All n-type implant dopants P, As and Sb showed higher dopant activation in Ge than Si for the same annealing temperature due to higher mobility and possible higher solid solubility limit. Severe surface dopant loss was reduced when using a surface oxide cap prior to annealing but dopant segregation into oxide needs to be optimized. C co-implant damage created acceptors that compensated the P dopant level especially at the lower dose of 2E15/cm^2. Using a Si-cap for P implant allows high temperature n-type dopant activation with minimal diffusion for shallow n+ Ge junctions that can be used for Ge nMOS as proposed by Borland in 2005 [12,13].

REFERENCES

[1] Saraswat, “Ge-based High-performance Nanoscale MOSFETs” presentation material from MRS April 2005 meeting.

[2] Kim et al., “Activation of Implanted n-Type Dopants in Ge Over the Active Concentration of 1x10^{20} cm^{-3} Using Coimplantation of Sb and P”, Electrochem and Solid-State Let., 13 (1) H12-H15 (2010).

[3] Trumble, “Solid Solubilities of Impurity Elements in Germanium and Silicon”, ECS May 1959 Philadelphia meeting.

[4] Private communication with K. Suguro of Toshiba, Sept 2013.

[5] Markevich et al., “Vacancy-group-V-impurity atom pairs in Ge crystals doped with P, As, Sb and Bi”, Physical Review B 70, 235213 (2004).

[6] Mazzocchi et al., “Boron and Phosphorus dopant activation in germanium using Laser annealing with and without preamorphization implant”, IEEE RTP-2009, p.141.

[7] Impellizzeri et al., “B activation and clustering in ion-implanted Ge”, Jour. App. Phy., vol. 105 (6), March 2009, p.63533-1.

[8] Borland et al., “Selective and Homo Emitter Junction Formation Using Precise Dopant Concentration Control by Ion Implantation and Microwave, Laser or Furnace Annealing Technique”, IEEE-PVSC June 2012 paper 626.

[9] Clarysse et al., “Active dopant characterization methology for germanium”, Jour. Vac. Sci. Tech. B., Vol 24 (1) Jan/Feb 2006, p. 381.

[10] Oh and Campell, “Thermal Desorption of Ge Native Oxides and the Loss of Ge from the Surface”, Jour. of Electronic Mat, vol. 33, No.4, 2004, p.364.

[11] Thareja et al., “High Performance Germanium N-MOSFET with Antimony Dopant Activation Beyond 1x10^{20}cm^{-3}”, IEDM-2010, paper 10.5, p.245.

[12] Borland et al., “Meeting challenges for engineering the gate stack”, Solid State Technology, July 2005, p.45.

[13] Borland et al., “Method of Forming Doped and Undoped Strained Semiconductor Materials and Films by Gas-Cluster-Ion-Beam Irradiation and Materials and Film Products”, US Patent#7,259,036 Aug 2007.